

A Ridge Penalized Likelihood Ratio Chart for Phase II Monitoring of High-Dimensional Process Dispersion Under Measurement System Inaccuracy

Esmaeil Safikhani¹, Ali Salmasnia^{2*} & Mohammad Reza Maleki³

Received 30 April 2022; Revised 20 May 2023; Accepted 27 May 2023;
© Iran University of Science and Technology 2023

ABSTRACT

In some applications, the number of quality characteristics is larger than the number of observations within subgroups. Common multivariate control charts to monitor the variability of such high-dimensional processes are unsuitable because the sample covariance matrix is not positive semi-definite and invertible. Moreover, the impact of gauge imprecision on detection capability of multivariate control charts under high-dimensional setting has been clearly neglected in the literature. To overcome these shortcomings, this paper develops a ridge penalized likelihood ratio chart for Phase II monitoring of high-dimensional process in the presence of measurement system errors. The developed control chart departs from the assumption of sparse variability shifts in which the assignable cause can only affect a few elements of the covariance matrix. Then, to compensate for the adverse impact of gauge impression, the developed chart is extended by employing multiple measurements on each sampled item. Simulation studies are carried out to study the impact of imprecise measurements on detectability of the developed monitoring scheme under different shift patterns. The results show that the gauge inability negatively affects the run-length distribution of the developed control chart. It is also found that the extended chart under multiple measurements strategy can effectively reduce the error impact.

KEYWORDS: High-dimensional process; Covariance matrix; Measurement errors; Ridge penalized likelihood ratio statistic; Multiple measurements per item.

1. Introduction

In today's competitive markets, companies are increasingly focusing on a large number of process quality characteristics to keep their market share, enhance customer satisfaction, and keep ahead of competition. Fortunately, the recent advances in data acquisition technologies have provided the possibility of collecting a great deal of information regarding quality characteristics of interest. On the other hand, data analysis obtained from each sample in processes

with a large number of quality characteristics entails a considerable amount of time and cost. In such situation, taking large samples has two main drawbacks: (1) it imposes a severe cost on manufacturer; (2) in manufacturing systems with low production speed, it is not possible to wait until a sufficient sample size be collected. Consequently, the quality practitioners may face conditions in which the number of process quality characteristics is larger than the sample size called "high-dimensionality". In this regard, [1] developed an improved version of the generalized T^2 chart based on random matrix theory for Phase II monitoring of high-dimensional; process mean. [2] integrated a divide-and-conquer strategy and multivariate exponentially weighted moving average (MEWMA) statistic for monitoring high-dimensional processes in which normality assumption of quality characteristics is relaxed

* Corresponding author: *Ali Salmasnia*
a.salmasnia@gom.ac.ir

1. Department of Industrial Engineering, University of Eyvanekey, Semnan, Iran.
2. Department of Industrial Engineering, Faculty of Engineering, University of Qom, Iran.
3. Industrial Engineering Group, Golpayegan College of Engineering, Isfahan University of Technology, Golpayegan 87717-67498, Iran.

[3] presented an integrated monitoring and diagnosis method based on principal component analysis (PCA) for high-dimensional data streams.

Using commonplace control charts to monitor the variability of high-dimensional processes is challenging because the sample covariance matrix is not positive semi-definite and its determinant tends toward zero. To overcome this problem, [4] proposed a novel algorithm based on parallelized Monte-Carlo simulation to enhance the sensitivity of two memory-type control charts for monitoring the variability of high dimensional processes. They employed different techniques for decreasing the computing space and run time. An adaptive LASSO-thresholding-based control chart for Phase II monitoring of multivariate normal quality characteristics under high-dimensional setting was suggested by [5] suggested. Using different out-of-control patterns, they confirmed the superiority of their proposed control chart over existing control charts. In contrast to the above-mentioned studies, [6] focused on detection of general changes in covariance matrix elements without sparsity assumption in Phase II monitoring of high-dimensional process variability. [7] extended the LASSO-thresholding-based control chart for Phase I monitoring of multivariate processes in condition that the process dimension is larger than the sample size. Using a real industrial data from the process of spur gear production, they validated the applicability of their proposed control chart. [8] gave the idea of tracking changes in sparse leading eigenvalue between two covariance matrices and studied Phase I monitoring high-dimensional process variability. [9] integrated ridge penalized likelihood ratio (RPLR) statistic and multiple dependent state sampling (MDS) strategy for monitoring high-dimensional covariance matrices. Then, they presented an improved version of the developed monitoring scheme based on generalized multiple dependent state sampling. The adverse effect of gauge inaccuracy on the performance of the adaptive thresholding LASSO control charting method for monitoring high-dimensional process variability was evaluated by [10]. They showed that the developed charting method has a better performance than the entropy chart in both with and without measurement error conditions. [11] equipped the adaptive thresholding LASSO chart with double sampling (DS) strategy for improving the chart sensitivity in reacting to

deviations of covariance matrix elements from their nominal values.

A vital issue affecting the performance of multivariate control charts is the ability of measurement system to accurately measure the quality characteristics of interest. Although some sources of uncertainty caused by the measurement devices always exist in reality, most existing control charts have been established based on the assumption of precise measurements. The existence of measurement error which is defined as the difference between the accurate and measured values of the process quality characteristics can significantly affects the performance of control charts. Consequently, it is crucial to develop the chart statistic by: (1) taking the measurement error component into account; (2) employing remedial strategies to reduce the impact of measurement inaccuracy on chart performance. Fortunately, the impact of measurement errors on detection capability of control charts have been well documented by recent studies such as [12-17]. More specifically, in the context of multivariate control charts, [18] used a linearly covariate error model and probed the impact of imprecise measurements on sensitivity of the variable sampling intervals (VSI) Hotelling's T^2 control chart. The impact of gauge measurement errors using a linear covariate model on the performance of the Hotelling CoDa (Compositional Data) T^2 control chart was studied by [19-20] studied the influence of gauge measurement errors on the performance of some one-sided variable sampling interval (VSI) EWMA-based control charts to monitor the multivariate coefficient of variation. More studies can be found in [21-25]. Interested readers can refer to review paper provided by [26].

This paper proposes a ridge penalized likelihood ratio chart with five important features: (1) it can be employed to monitor multivariate process variability when the process dimension exceeds the sample size; (2) it departs from the assumption of sparse in-control covariance matrix; (3) in contrast to the existing charts for monitoring high-dimensional process variability that are only applicable for sparse changes, it can be used for detecting general shift patterns in the original variability matrix; (4) it takes the existence of gauge imprecision into account; and (5) it develops multiple measurements strategy to compensate for the undesired impact of error variance on chart performance. Note that, sparse variability changes is referred to condition that

only few covariance matrix elements are simultaneously effected by assignable. The structure of this paper is organized as follows: The ridge penalized likelihood ratio statistic considering an additive covariate model is developed in Section 2. To reduce the undesired impact of contaminated data due to gauge impression, the developed chart is extended on the basis of multiple measurements strategy in Section 3. Simulation studies in terms of run length properties are conducted in Section 4 to compare the detection capability of the ridge penalized likelihood ratio chart under with and without errors scenarios. Ultimately, Section 5 furnishes the conclusions of our proposed charts and provides some recommendations for future studies.

2. RPLRME Control Chart

In this section, a control chart for Phase II monitoring of high-dimensional process variability is developed based on the ridge penalized likelihood ratio statistic under the gauge measurement errors. The developed chart hereafter called RPLRME chart has the following advantages: (1) considering general covariance matrix shift patterns without the sparsity assumption, (2) detecting covariance matrix abnormalities even when the process dimension exceed the subgroup size, (3) taking into account the gauge inability to accurately measure the value of process quality characteristics, and (4) presenting a closed form to estimate the precision matrix in contrast to the conventional penalized likelihood ratio-based charts which suffer from complex computational procedures. In this regard, first the variables and parameters used to establish the RPLRME chart are summarized in Table 1.

Tab. 1. Notations

| Notation | Description |
|--------------------------------|---|
| Indices | |
| t | Index of subgroups |
| i | Index of observations |
| j, k | Index of quality characteristics |
| r | Index of measurements per item |
| Distribution parameters | |
| \mathbf{X}_t | Accurate values matrix of observations in subgroup t |
| \mathbf{x}_i | i^{th} observation vector of quality characteristics in subgroup t |
| x_{ijk} | i^{th} observation of j^{th} quality characteristic in subgroup t |
| p | Number of quality characteristics |
| $\boldsymbol{\mu}_x$ | Mean vector of \mathbf{X}_t |
| $\boldsymbol{\Sigma}_x$ | Covariance matrix of \mathbf{X}_t |
| $\boldsymbol{\Sigma}_{x,ic}$ | In-control covariance matrix of \mathbf{X}_t |
| $\boldsymbol{\Sigma}_{x,oc}$ | Out-of-control covariance matrix of \mathbf{X}_t |
| σ_{jk} | Covariance of quality characteristics j and k |
| σ_j^2 | Variance of j^{th} quality characteristic |
| Chart parameters | |
| α | Probability of Type I error |
| n | Sample size |
| θ | Tuning parameter |
| $RPLRME$ | Statistic of ridge penalized likelihood ratio with measurement errors |
| $RPLRMME$ | Statistic of ridge penalized likelihood ratio under multiple measurements |
| UCL_{RPLRME} | Upper control limit of RPLRME chart |
| $UCL_{RPLRMME}$ | Upper control limit of RPLRMME chart |

| Error parameters | |
|---|---|
| $\boldsymbol{\varepsilon}_t$ | Error terms matrix in subgroup t |
| $\boldsymbol{\varepsilon}_{it}$ | The i^{th} column of $\boldsymbol{\varepsilon}_t$ |
| $\boldsymbol{\mu}_\varepsilon$ | Mean vector of $\boldsymbol{\varepsilon}_{ij}$ |
| $\boldsymbol{\Sigma}_\varepsilon$ | Covariance matrix of $\boldsymbol{\varepsilon}_{ij}$ |
| $\sigma_{\varepsilon,j}^2$ | Variance of error term related to quality characteristic j |
| \mathbf{A} | Intercept coefficients vector of multivariate additive covariate model |
| \mathbf{B} | Slope coefficients vector of multivariate additive covariate model |
| \mathbf{Y}_t | Measured values matrix of observations in subgroup t |
| $\boldsymbol{\mu}_Y = \mathbf{A} + \mathbf{B}\boldsymbol{\mu}_X$ | Mean vector of \mathbf{Y}_t |
| $\boldsymbol{\Sigma}_Y = \mathbf{B}\boldsymbol{\Sigma}_X\mathbf{B}^T + \boldsymbol{\Sigma}_\varepsilon$ | Covariance matrix of \mathbf{Y}_t |
| $\boldsymbol{\Sigma}_{Y,ic}$ | In-control covariance matrix of \mathbf{Y}_t |
| $\boldsymbol{\Omega}$ | Precision matrix of \mathbf{Y}_t |
| $\boldsymbol{\Omega}_{ic}$ | In-control precision matrix of \mathbf{Y}_t |
| $\boldsymbol{\Omega}_{ic}^m$ | In-control precision matrix of $\bar{\mathbf{Y}}_t$ |
| $\hat{\boldsymbol{\Omega}}_t^{MLE}$ | Estimated precision matrix of \mathbf{Y}_t based on MLE |
| $\hat{\boldsymbol{\Omega}}_t^{RPLRME}$ | Estimated precision matrix of \mathbf{Y}_t based on RPLRME |
| $\hat{\boldsymbol{\Omega}}_t^{RPLRMME}$ | Estimated precision matrix of $\bar{\mathbf{Y}}_t$ based on RPLRMME |
| m | Number of measurements on a given item |
| Others | |
| \mathbf{S}_t | Sample covariance matrix in subgroup t |
| \mathbf{S}_t^m | Sample covariance matrix in subgroup t under multiple measurements per item |
| ARL_{ic} | In-control average run length |
| ARL_{oc} | Out-of-control average run length |
| $SDRL_{ic}$ | In-control standard deviation of run length |
| $SDRL_{oc}$ | Out-of-control standard deviation of run length |
| τ | Sampling interval in which an assignable cause occurs |
| T | Sampling interval in which the chart signals an out-of-control signal |

Let $\mathbf{X}_t = (\mathbf{x}_{t1}, \mathbf{x}_{t2}, \dots, \mathbf{x}_{tm})_{p \times n}; t = 1, 2, \dots, T$ be a $p \times n$ matrix of observations collected at t^{th} sampling point in which the i^{th} observation denoted as $\mathbf{x}_{it} = (x_{ij1}, x_{ij2}, \dots, x_{ijp})^T; i = 1, \dots, n$ follows a p -variate normal distribution. The occurrence of assignable causes at sampling point τ changes the process covariance matrix from

$\boldsymbol{\Sigma}_X^{ic}$ to $\boldsymbol{\Sigma}_X^{oc}$. In fact, for subgroups $t = 1, 2, \dots, \tau$, the process parameters remain in-control i.e., $\mathbf{x}_{it} \sim MVN(\boldsymbol{\mu}_X, \boldsymbol{\Sigma}_X^{ic})$ whereas we have $\mathbf{x}_{it} \sim MVN(\boldsymbol{\mu}_X, \boldsymbol{\Sigma}_X^{oc})$ at sampling points $t = \tau + 1, \dots, T$. In this study, we consider an additive covariate model to associate the accurate values of quality characteristics with their corresponding measured values as:

$$\mathbf{Y}_t = \mathbf{A} + \mathbf{B}\mathbf{X}_t + \boldsymbol{\varepsilon}_t \quad (1)$$

where $\mathbf{Y}_t = (\mathbf{y}_{t1}, \mathbf{y}_{t2}, \dots, \mathbf{y}_{tm})_{p \times n}$ denotes the matrix of measured quality characteristics at t^{th} sampling stage while $\mathbf{A} = (a_1, a_2, \dots, a_p)^T$ and

$$\mathbf{B} = \begin{pmatrix} b_1 & 0 & \dots & 0 \\ 0 & b_2 & \dots & 0 \\ \vdots & \vdots & \ddots & \vdots \\ 0 & 0 & \dots & b_p \end{pmatrix}_{p \times p} \quad \text{contain constant}$$

intercept and slope error model parameters, respectively. Moreover, $\boldsymbol{\varepsilon}_t = (\boldsymbol{\varepsilon}_{t1}, \boldsymbol{\varepsilon}_{t2}, \dots, \boldsymbol{\varepsilon}_{tm})_{p \times n}$ represents the matrix of error values which

$$\boldsymbol{\mu}_Y = \mathbf{A} + \mathbf{B}\boldsymbol{\mu}_X \quad (2)$$

$$\boldsymbol{\Sigma}_Y = \mathbf{B}\boldsymbol{\Sigma}_X\mathbf{B}^T + \boldsymbol{\Sigma}_\varepsilon = \begin{pmatrix} b_1^2\sigma_1^2 + \sigma_{\varepsilon,1}^2 & b_1b_2\sigma_{12} & \dots & b_1b_p\sigma_{1p} \\ b_2b_1\sigma_{12} & b_2^2\sigma_2^2 + \sigma_{\varepsilon,2}^2 & \dots & b_2b_p\sigma_{2p} \\ \vdots & \vdots & \ddots & \vdots \\ b_pb_1\sigma_{1p} & b_pb_2\sigma_{2p} & \dots & b_p^2\sigma_p^2 + \sigma_{\varepsilon,p}^2 \end{pmatrix}_{p \times p} \quad (3)$$

In order to estimate the precision matrix $\boldsymbol{\Omega}$, the likelihood function at t^{th} sampling stage given the vectors $\mathbf{y}_{t1}, \mathbf{y}_{t2}, \dots, \mathbf{y}_{tm}$ is constructed as:

$$f(\mathbf{y}_{t1}, \dots, \mathbf{y}_{tm} | \boldsymbol{\Omega}) = (2\pi n)^{-\frac{np}{2}} |\boldsymbol{\Omega}|^{-\frac{1}{2}} e^{-\sum_{i=1}^n (\mathbf{y}_{ti} - \boldsymbol{\mu}_Y)^T \boldsymbol{\Omega} (\mathbf{y}_{ti} - \boldsymbol{\mu}_Y)} \quad (4)$$

where $\boldsymbol{\Omega} = \boldsymbol{\Sigma}_Y^{-1}$. The maximum likelihood estimator (MLE) of precision matrix can be estimated by solving the optimization problem as below:

$$\hat{\boldsymbol{\Omega}}_t^{MLE} = \arg \min_{\boldsymbol{\Omega}} \{tr(\boldsymbol{\Omega}\mathbf{S}_t) - \log|\boldsymbol{\Omega}|\} \quad (5)$$

where $\mathbf{S}_t = \frac{1}{n} \sum_{i=1}^n (\mathbf{y}_{ti} - \boldsymbol{\mu}_Y)(\mathbf{y}_{ti} - \boldsymbol{\mu}_Y)^T$ denotes the sample covariance matrix for t^{th} random subgroup. For sampling stage $t; t=1, \dots, T$, the optimum solution of the mathematical programming (5) will be equal to the inverse of the sample covariance matrix as $\hat{\boldsymbol{\Omega}}_t^{MLE} = \mathbf{S}_t^{-1}$. However, using MLE approach to estimate the

follows a p -variate normal distribution with parameters $\boldsymbol{\mu}_\varepsilon = (0, 0, \dots, 0)^T$,

$$\boldsymbol{\Sigma}_\varepsilon = \begin{pmatrix} \sigma_{\varepsilon,1}^2 & 0 & \dots & 0 \\ 0 & \sigma_{\varepsilon,2}^2 & \dots & 0 \\ \vdots & \vdots & \ddots & \vdots \\ 0 & 0 & \dots & \sigma_{\varepsilon,p}^2 \end{pmatrix} \quad \text{and is independent}$$

from \mathbf{X}_t . According to Equation (1), $\mathbf{y}_{ti}; i=1, \dots, n$

follows a p -variate normal distribution with mean vector $\boldsymbol{\mu}_Y$ and covariance matrix $\boldsymbol{\Sigma}_Y$ as:

precision matrix is inapplicable when p is larger than n because \mathbf{S}_t is not invertible. For two reasons of: (1) shrinking the unchanged elements in $\boldsymbol{\Sigma}_Y$ to the corresponding ones in $\boldsymbol{\Sigma}_{Y,ic}$; and (2) overcoming the invertibility limitation of the estimated precision matrix, the L_2 penalty term is added to mathematical programming (5) by taking the idea of ridge penalized likelihood ratio (RPLR) procedure. Based on this procedure, the precision matrix of high-dimensional process under measurement errors denoted by $\hat{\boldsymbol{\Omega}}_t^{RPLRME}$ can be estimated as:

$$\hat{\boldsymbol{\Omega}}_t^{RPLRME} = \arg \min_{\boldsymbol{\Omega}} \left\{ tr(\boldsymbol{\Omega}\mathbf{S}_t) - \log|\boldsymbol{\Omega}| + \frac{\theta}{2} \|\boldsymbol{\Omega} - \boldsymbol{\Omega}_{ic}\| \right\} \quad (6)$$

where $\boldsymbol{\Omega}_{ic} = \boldsymbol{\Sigma}_{Y,ic}^{-1}$ and $\theta; \theta > 0$ is a tuning parameter which is employed to obtain various levels of shrinkage of $\hat{\boldsymbol{\Omega}}_t^{RPLRME}$. Based on the mathematical programming (6), $\hat{\boldsymbol{\Omega}}_t^{RPLRME}$ can be attained according to Equation (7).

$$\hat{\Omega}_t^{RPLRME} = \left\{ \left(\theta \mathbf{I}_p + \frac{1}{4} (\mathbf{S}_t - \theta \Omega_{ic})^2 \right)^{\frac{1}{2}} + \frac{1}{2} (\mathbf{S}_t - \theta \Omega_{ic}) \right\}^{-1} \quad (7)$$

It can be concluded from Equation (7) that $\hat{\Omega}_t^{RPLRME}$ tends toward Ω_{ic} when $\theta \rightarrow \infty$ while in situation that $\theta \rightarrow 0$, $\hat{\Omega}_t^{RPLRME}$ approaches \mathbf{S}_t^{-1} . Determining the status of high-dimensional process variability under gauge measurement errors is equivalent to conducting the following hypothesis test:

$$RPLRME_t = tr(\Omega_{ic} \mathbf{S}_t) + \ln |\hat{\Omega}_t^{RPLRME}| - \ln |\Omega_{ic}| - tr(\hat{\Omega}_t^{RPLRME} \mathbf{S}_t) \quad (9)$$

The RPLRME chart issues an out-of-control signal whenever $RPLRME_t > UCL_{RPLRME}$ where the value of UCL_{RPLRME} is selected so that the in-control average run length (ARL_{ic}) be equal to $\frac{1}{\alpha}$. Note that the average run length is defined as the expected value of a run length random variable which specifies the number of samples till issuing an out-of-control signal.

3. RPLRME Control Chart Under Multiple Measurements Approach

In order to increase the chart detectability and get more robust results, the undesired impact of gauge imprecision should be diminished by employing remedial approaches. In this regard, multiple measurements strategy as one of the most efficient remedial methods was proposed by [27] and has been employed in some other studies such as [28-30]. Taking multiple measurements on each sampled point instead of individual ones enhances the chart sensitivity due to reduction of

$$\begin{aligned} H_0 : \Sigma_Y &= \mathbf{B} \Sigma_{X,ic} \mathbf{B}^T + \Sigma_\varepsilon \\ H_1 : \Sigma_Y &\neq \mathbf{B} \Sigma_{X,ic} \mathbf{B}^T + \Sigma_\varepsilon \end{aligned} \quad (8)$$

For t^{th} random sample, the developed statistic based on the integration of the ridge penalized likelihood ratio estimator and the measurement errors (RPLRME) can be written as:

the extra variability caused by error term. Based on this, a novel control chart hereafter called RPLRMME is established by extending the RPLRME chart under multiple measurements strategy. Let $\bar{\mathbf{Y}}_t = (\bar{\mathbf{y}}_{t1}, \bar{\mathbf{y}}_{t2}, \dots, \bar{\mathbf{y}}_{tm})_{p \times n}$ denotes the observations taken at the t^{th} subgroup where each sample unit is inspected $m; m > 1$ times. Besides, $\bar{\mathbf{y}}_{ii} = (\bar{y}_{ii1}, \bar{y}_{ii2}, \dots, \bar{y}_{iip})^T$ represents the elements of the i^{th} column of observations matrix $\bar{\mathbf{Y}}_t$ where

$\bar{y}_{ij} = \frac{\sum_{r=1}^m y_{ijr}}{m}$. It can be statistically checked that $\bar{\mathbf{y}}_{ii}$ follows a p -variate normal distribution with mean vector $\boldsymbol{\mu}_{\bar{\mathbf{y}}} = \mathbf{A} + \mathbf{B} \boldsymbol{\mu}_X$ and covariance matrix $\Sigma_{\bar{\mathbf{y}}} = \mathbf{B} \Sigma_X \mathbf{B}^T + \frac{\Sigma_\varepsilon}{m}$. Accordingly, the covariance matrix of $\bar{\mathbf{y}}_{ii}$ can be rewritten as:

$$\Sigma_{\bar{\mathbf{y}}} = \begin{pmatrix} b_1^2 \sigma_{11} + \frac{\sigma_{\varepsilon,1}^2}{m} & b_1 b_2 \sigma_{12} & \dots & b_1 b_p \sigma_{1p} \\ b_2 b_1 \sigma_{12} & b_2^2 \sigma_{22} + \frac{\sigma_{\varepsilon,2}^2}{m} & \dots & b_2 b_p \sigma_{2p} \\ \vdots & \vdots & \ddots & \vdots \\ b_p b_1 \sigma_{1p} & b_p b_2 \sigma_{2p} & \dots & b_p^2 \sigma_{pp} + \frac{\sigma_{\varepsilon,p}^2}{m} \end{pmatrix}_{p \times p} \quad (10)$$

The likelihood function under taking m measurements on each sampled item is constructed by replacing \mathbf{y}_{ii} by $\bar{\mathbf{y}}_{ii}$ in Equation

(4). For t^{th} random sample, the estimation of precision matrix to construct the RPLEMME chart is:

$$\hat{\Omega}_t^{RPLRMME} = \underset{\Omega}{\operatorname{argmin}} \left\{ \operatorname{tr}(\Omega \mathbf{S}_t^m) - \log |\Omega| + \frac{\theta}{2} \|\Omega - \Omega_{ic}^m\| \right\} \quad (11)$$

where $\mathbf{S}_t^m = \frac{1}{n} \sum_{i=1}^n (\bar{\mathbf{y}}_{ti} - \boldsymbol{\mu}_{\bar{\mathbf{y}}}) (\bar{\mathbf{y}}_{ti} - \boldsymbol{\mu}_{\bar{\mathbf{y}}})^T$.

Equivalently, we can write:

$$\hat{\Omega}_t^{RPLRMME} = \left\{ \left(\theta \mathbf{I}_p + \frac{1}{4} (\mathbf{S}_t^m - \theta \Omega_{ic}^m)^2 \right)^{\frac{1}{2}} + \frac{1}{2} (\mathbf{S}_t^m - \theta \Omega_{ic}^m) \right\}^{-1} \quad (12)$$

$$RPLRMME_t = \operatorname{tr}(\Omega_{ic}^m \mathbf{S}_t^m) + \ln |\hat{\Omega}_t^{RPLRMME}| - \ln |\Omega_{ic}^m| - \operatorname{tr}(\hat{\Omega}_t^{RPLRMME} \mathbf{S}_t^m) \quad (13)$$

A signal is triggered by The RPLRMME if $RPLRMME_t > UCL_{RPLRMME}$ where the value of $UCL_{RPLRMME}$ is set based on simulation experiments to achieve a pre-determined ARL_{ic} .

4. Performance Comparison

In this section, the impact of inaccurate measurements on efficiency of the RPLR chart is investigated based on Monte Carlo simulations. Consider a multivariate process in which the product quality is characterized via $p = 10$ normally distributed variables. It is assumed that $\boldsymbol{\Sigma}_{x,ic} = \mathbf{I}_{10}$ when the process is in-control. The parameters of the RPLRME chart are selected as $n = 5$ and $\theta = 10$. We consider an additive covariate model with constant values of $\mathbf{A} = \mathbf{0}_{10 \times 1}$

$$\sigma_j^2 = 1 + \delta^2; j = 1, \dots, 10 \text{ and } \sigma_{jk} = \delta; j, k = 1, \dots, 10 \text{ \& } j \neq k \quad (14)$$

Scenario 2: The second out-of-control scenario is similar to the first scenario with this difference

$$\sigma_j^2 = 1 + \delta^2; j = 1, \dots, 5 \text{ and } \sigma_{jk} = \delta; j, k = 1, \dots, 5 \text{ \& } j \neq k \quad (15)$$

Scenario 3: In this condition, the variance and covariance elements of the first and second variables are affected as Equation (16):

$$\sigma_j^2 = 1 + \delta^2; j = 1, 2 \text{ and } \sigma_{12} = \sigma_{21} = \delta \quad (16)$$

Scenario 4: As given in Equation (17), the occurrence of assignable cause affects all variance elements while the covariance elements remain unchanged.

Using RPLRMME chart for Phase II monitoring of high-dimensional process variability is equivalent to test the null hypothesis

$$H_0 : \boldsymbol{\Sigma}_{\bar{\mathbf{y}}} = \mathbf{B} \boldsymbol{\Sigma}_0 \mathbf{B}^T + \frac{\boldsymbol{\Sigma}_\varepsilon}{m} \text{ versus the alternative}$$

$$\text{one } H_1 : \boldsymbol{\Sigma}_{\bar{\mathbf{y}}} \neq \mathbf{B} \boldsymbol{\Sigma}_0 \mathbf{B}^T + \frac{\boldsymbol{\Sigma}_\varepsilon}{m} . \text{ The developed}$$

chart statistic at the t^{th} sampling stage is given as:

and $\mathbf{B} = \mathbf{I}_{10}$ in which

$$\sigma_{\varepsilon,j}^2 = \sigma_\varepsilon^2; \sigma_\varepsilon^2 \in \{0, 0.05, 0.1, 0.15, 0.2, 0.25\} \text{ for } j = 1, \dots, 10 . \text{ It is worth mentioning that the case}$$

$\sigma_\varepsilon^2 = 0$ implies that the observations are collected under without measurement errors condition. For each value of σ_ε^2 , the

$UCL_{RPLRMME}$ is set subject to $ARL_{ic} = 200$. Then, the sensitivity of the RPLRME chart under seven out-of-control scenarios is evaluated in terms of ARL_{oc} and $SDRL_{oc}$. These scenarios include diagonal, off-diagonal as well as concurrent diagonal/off-diagonal disturbances as follows:

Scenario 1: The occurrence of assignable cause leads to shifts in all covariance matrix elements as follows:

that the assignable cause affects the variance and covariance elements of the first five variables.

$$\sigma_j^2 = 1 + \delta^2; j = 1, \dots, 10 \quad (17)$$

Scenario 5: The out-of-control condition is restricted to only the variance of the first variable. In other words, the other variance/covariance elements remain unchanged:

$$\sigma_1^2 = 1 + \delta^2 \quad (18)$$

Scenario 6: As seen in Equation (19), the out-of-control covariance matrix includes off-diagonal disturbances related to the first five variables.

$$\sigma_{jk} = \delta; j, k = 1, \dots, 5 \text{ \& } j \neq k \quad (19)$$

Scenario 7: This scenario is similar to the previous scenario with this difference that the assignable cause changes the covariance of the first and second variables.

$$\sigma_{12} = \sigma_{21} = \delta \quad (20)$$

The resulting *ARLs* and *SDRLs* of the developed RPLRME chart for both with and without error cases under the mentioned out-of-control scenarios when $\delta \in \{0, 0.1, 0.2, 0.3, 0.5, 0.75, 1\}$ are presented in Tables 2-8. As seen from Tables 2-8, the gauge measurement errors diminishes the detecting capability of the developed RPLRME chart to react to the sustained changes in covariance matrix elements. It can be confirmed from Tables 2-8 that the *ARL* and *SDRL* values increase as the error variance increases. That is to say that the larger value of σ_ϵ^2 , the larger values of both ARL_{oc} and $SDRL_{oc}$. Specifically, it can be observed from Table 2 that for $\delta = 0.1$, the chart obtains $ARL_{oc} = 71.8085$ when the measurements are accurate. However, the existence of measurement errors increases the value of ARL_{oc} to 78.2490, 84.9975, 89.4355, 95.9365, and 96.1550 when σ_ϵ^2 equals to 0.05, 0.1, 0.15, 0.2, and 0.25, respectively. In other words, for $\delta = 0.1$, increasing the error variance to 0.05, 0.1, 0.15, 0.2, and 0.25 leads to reducing the chart sensitivity about 8.97, 18.37, 24.55, 33.60, and 33.90 percent, respectively, when the covariance matrix elements are affected according to the first out-of-control scenario. The results of Table 3 indicate that both the values of ARL_{oc} and $SDRL_{oc}$ in scenario 2 are always larger than those of scenario 1. This is due to the fact that, in spite of the first scenario, the assignable cause affects 25 percent of the covariance matrix elements in the second scenario. For instance under the second scenario, when $\sigma_\epsilon^2 = 0.1$ and $\delta = 0.3$, the developed chart

obtains $ARL_{oc} = 41.1420$ which is remarkably larger than that of the first scenario, i.e. $ARL_{oc} = 9.8935$. It can be also concluded from comparing the results of Tables 2-4 that the capability of the developed chart to detect covariance matrix anomalies significantly reduces when the assignable cause affects the process variability according to the third out-of-control scenario.

Table 5 reveals that as the error variance increases from 0 to 0.25, the efficiency of the RPLRME control chart to detect diagonal covariance matrix shifts reduces, dramatically. For instance, for $\delta = 0.5$, increasing the error variance from 0.05 to 0.25 result in increasing the value of ARL_{oc} from 14.3550 to 18.7240. That is to say, under the mentioned condition, the detection capability of the RPLRME chart degrades about 30.43 percent. Besides, the impact of off-diagonal shifts on detection performance of the developed chart can be disclosed by comparing the results of Tables 2 and 5. For more clarification, under the case $\sigma_\epsilon^2 = 0.1$ when $\delta = 0.5$, we have $ARL_{oc} = 3.6375$ when both diagonal and off-diagonal are affected by the assignable cause while the RPLRME chart detects the sustained shift in diagonal elements after average of 15.5630 samples. The results of Tables 6 and 8 tells us that in contrast to the other charts developed for monitoring high-dimensional processes, the proposed RPLRME scheme can detect sparse shifts when only few number of covariance matrix elements are changed. However, as expected, the occurrence of such shifts is detected with a delay when the magnitude of shift is small. It is clear from the values of *ARLs* and *SDRLs* shown in Table 7 that similar to the previous out-of-control scenarios, the existence of measurement error causes a delay in the detection of shift when only off-diagonal elements change from their nominal values.

Tab. 2. ARL and SDRL comparison under different error variance values in scenario 1

| δ | Criterion | UCL_{RPLRME} | | | | | |
|----------|-------------|-------------------------|----------------------------|---------------------------|----------------------------|---------------------------|----------------------------|
| | | 4.8104 | 5.1018 | 5.3913 | 5.6462 | 5.8613 | 6.0642 |
| | | $\sigma_\epsilon^2 = 0$ | $\sigma_\epsilon^2 = 0.05$ | $\sigma_\epsilon^2 = 0.1$ | $\sigma_\epsilon^2 = 0.15$ | $\sigma_\epsilon^2 = 0.2$ | $\sigma_\epsilon^2 = 0.25$ |
| 0 | <i>ARL</i> | 200.0270 | 200.3655 | 200.6080 | 200.2390 | 200.0824 | 199.2450 |
| | <i>SDRL</i> | 198.3768 | 202.8921 | 203.3510 | 199.1435 | 202.0609 | 202.5535 |
| 0.1 | <i>ARL</i> | 71.8085 | 78.2490 | 84.9975 | 89.4355 | 95.9365 | 96.1550 |
| | <i>SDRL</i> | 69.2305 | 75.6523 | 83.7848 | 87.6284 | 95.5930 | 97.5912 |

| | | | | | | | |
|------|------|---------|---------|---------|---------|---------|---------|
| 0.2 | ARL | 18.9235 | 21.1540 | 23.9755 | 24.8830 | 28.4755 | 30.4290 |
| | SDRL | 18.5084 | 20.5907 | 22.9208 | 24.2471 | 28.5526 | 30.4888 |
| 0.3 | ARL | 7.9315 | 8.6975 | 9.8935 | 10.9760 | 12.0225 | 13.4650 |
| | SDRL | 7.5446 | 8.3050 | 9.8936 | 10.4862 | 11.4784 | 12.8001 |
| 0.50 | ARL | 3.2080 | 3.3755 | 3.6375 | 3.9580 | 4.0320 | 4.5755 |
| | SDRL | 2.6986 | 2.9492 | 3.0089 | 3.3062 | 3.4802 | 3.9587 |
| 0.75 | ARL | 1.7765 | 1.8815 | 1.9365 | 2.0780 | 2.1435 | 2.2315 |
| | SDRL | 1.2285 | 1.2966 | 1.4041 | 1.4846 | 1.5672 | 1.6713 |
| 1 | ARL | 1.3030 | 1.3510 | 1.4155 | 1.4745 | 1.4895 | 1.5155 |
| | SDRL | 0.6176 | 0.7043 | 0.7518 | 0.8501 | 0.8504 | 0.8923 |

Tab. 3. ARL and SDRL comparison under different error variance values in scenario 2

| δ | Criterion | UCL_{RPLRME} | | | | | |
|----------|-----------|------------------|---------------------|--------------------|---------------------|--------------------|---------------------|
| | | 4.8104 | 5.1018 | 5.3913 | 5.6462 | 5.8613 | 6.0642 |
| | | $\sigma_e^2 = 0$ | $\sigma_e^2 = 0.05$ | $\sigma_e^2 = 0.1$ | $\sigma_e^2 = 0.15$ | $\sigma_e^2 = 0.2$ | $\sigma_e^2 = 0.25$ |
| 0 | ARL | 200.0270 | 200.3655 | 200.6080 | 200.2390 | 200.0824 | 199.2450 |
| | SDRL | 198.3768 | 202.8921 | 203.3510 | 199.1435 | 202.0609 | 202.5535 |
| 0.1 | ARL | 151.7150 | 152.8570 | 158.2295 | 159.8290 | 160.9275 | 165.6505 |
| | SDRL | 156.9350 | 152.4835 | 154.4426 | 160.0299 | 160.4088 | 162.3510 |
| 0.2 | ARL | 73.4590 | 77.5315 | 84.9070 | 86.7075 | 94.6700 | 97.8320 |
| | SDRL | 75.5450 | 78.4171 | 82.8794 | 87.7331 | 95.1895 | 97.7902 |
| 0.3 | ARL | 33.2720 | 36.4045 | 41.1420 | 43.0160 | 46.2385 | 49.7135 |
| | SDRL | 33.1084 | 34.3605 | 40.1299 | 41.8369 | 46.8872 | 49.5135 |
| 0.5 | ARL | 10.2085 | 10.6500 | 12.3230 | 13.5325 | 14.4355 | 15.7470 |
| | SDRL | 9.6701 | 10.5633 | 11.9362 | 13.7195 | 13.7217 | 14.8825 |
| 0.75 | ARL | 3.9700 | 4.4025 | 4.5290 | 5.1435 | 5.5450 | 5.7540 |
| | SDRL | 3.3421 | 3.9340 | 4.1704 | 4.6375 | 4.9773 | 5.0501 |
| 1 | ARL | 2.2880 | 2.4870 | 2.5055 | 2.6805 | 2.8160 | 3.0440 |
| | SDRL | 1.7273 | 1.9702 | 1.9774 | 2.0299 | 2.2380 | 2.5104 |

Tab. 4. ARL and SDRL comparison under different error variance values in scenario 3

| δ | Criterion | UCL_{RPLRME} | | | | | |
|----------|-----------|------------------|---------------------|--------------------|---------------------|--------------------|---------------------|
| | | 4.8104 | 5.1018 | 5.3913 | 5.6462 | 5.8613 | 6.0642 |
| | | $\sigma_e^2 = 0$ | $\sigma_e^2 = 0.05$ | $\sigma_e^2 = 0.1$ | $\sigma_e^2 = 0.15$ | $\sigma_e^2 = 0.2$ | $\sigma_e^2 = 0.25$ |
| 0 | ARL | 200.0270 | 200.3655 | 200.6080 | 200.2390 | 200.0824 | 199.2450 |
| | SDRL | 198.3768 | 202.8921 | 203.3510 | 199.1435 | 202.0609 | 202.5535 |
| 0.1 | ARL | 182.4620 | 189.9020 | 191.1520 | 192.2425 | 193.5325 | 194.8600 |
| | SDRL | 177.0263 | 184.1790 | 191.2818 | 192.2316 | 194.6210 | 194.7752 |
| 0.2 | ARL | 167.4450 | 168.2690 | 170.4525 | 172.6790 | 174.1975 | 175.1330 |
| | SDRL | 167.1549 | 168.0785 | 168.1042 | 172.6253 | 174.1035 | 174.3643 |
| 0.3 | ARL | 134.4550 | 135.1255 | 137.6800 | 140.4765 | 142.0880 | 143.0055 |
| | SDRL | 131.0360 | 135.3170 | 138.0111 | 142.3586 | 140.4695 | 141.4138 |
| 0.50 | ARL | 62.5985 | 64.9740 | 71.8440 | 74.7880 | 75.4545 | 78.3770 |
| | SDRL | 64.5629 | 64.7282 | 70.1587 | 74.9071 | 75.5362 | 79.3273 |
| 0.75 | ARL | 23.3575 | 24.8950 | 27.0560 | 28.9930 | 30.9645 | 32.3025 |
| | SDRL | 22.7927 | 24.6502 | 26.9691 | 28.8862 | 30.0898 | 31.9370 |
| 1 | ARL | 9.1005 | 10.0330 | 10.6560 | 11.6480 | 12.7095 | 13.9965 |
| | SDRL | 8.6486 | 9.5330 | 9.9441 | 10.8227 | 12.4205 | 13.3382 |

Tab. 5. ARL and SDRL comparison under different error variance values in scenario 4

| δ | Criterion | UCL_{RPLRME} | | | | | |
|----------|-----------|------------------|---------------------|--------------------|---------------------|--------------------|---------------------|
| | | 4.8104 | 5.1018 | 5.3913 | 5.6462 | 5.8613 | 6.0642 |
| | | $\sigma_e^2 = 0$ | $\sigma_e^2 = 0.05$ | $\sigma_e^2 = 0.1$ | $\sigma_e^2 = 0.15$ | $\sigma_e^2 = 0.2$ | $\sigma_e^2 = 0.25$ |
| 0 | ARL | 200.0270 | 200.3655 | 200.6080 | 200.2390 | 200.0824 | 199.2450 |
| | SDRL | 198.3768 | 202.8921 | 203.3510 | 199.1435 | 202.0609 | 202.5535 |
| 0.1 | ARL | 181.3370 | 183.9370 | 184.1130 | 185.3660 | 186.0315 | 187.4475 |

| | | | | | | | |
|------|-------------|----------|----------|----------|-----------|----------|----------|
| | <i>SDRL</i> | 184.0674 | 184.4873 | 184.7206 | 185.5717 | 185.3361 | 187.5506 |
| 0.2 | <i>ARL</i> | 112.3760 | 118.1060 | 121.7320 | 121.89085 | 122.5630 | 123.8915 |
| | <i>SDRL</i> | 111.1317 | 118.6844 | 117.1182 | 123.3894 | 122.9964 | 123.4841 |
| 0.3 | <i>ARL</i> | 61.3020 | 61.8475 | 66.8410 | 69.9680 | 70.2390 | 70.8125 |
| | <i>SDRL</i> | 61.0218 | 61.8580 | 65.4398 | 69.6326 | 70.5960 | 70.6627 |
| 0.50 | <i>ARL</i> | 13.4815 | 14.3550 | 15.5630 | 16.6285 | 17.3055 | 18.7240 |
| | <i>SDRL</i> | 12.8838 | 14.3760 | 15.1277 | 16.3202 | 17.5520 | 18.4422 |
| 0.75 | <i>ARL</i> | 2.7455 | 2.9370 | 3.1570 | 3.3265 | 3.5515 | 3.8760 |
| | <i>SDRL</i> | 2.1310 | 2.4333 | 2.6015 | 2.9078 | 2.9405 | 3.3017 |
| 1 | <i>ARL</i> | 1.2635 | 1.3225 | 1.3535 | 1.4650 | 1.4740 | 1.5370 |
| | <i>SDRL</i> | 0.5632 | 0.6471 | 0.6977 | 0.8081 | 0.8314 | 0.8860 |

Tab. 6. ARL and SDRL comparison under different error variance values in scenario 5

| δ | Criterion | UCL_{RPLRME} | | | | | |
|----------|-------------|-------------------------|----------------------------|---------------------------|----------------------------|---------------------------|----------------------------|
| | | 4.8104 | 5.1018 | 5.3913 | 5.6462 | 5.8613 | 6.0642 |
| | | $\sigma_\epsilon^2 = 0$ | $\sigma_\epsilon^2 = 0.05$ | $\sigma_\epsilon^2 = 0.1$ | $\sigma_\epsilon^2 = 0.15$ | $\sigma_\epsilon^2 = 0.2$ | $\sigma_\epsilon^2 = 0.25$ |
| 0 | <i>ARL</i> | 200.0270 | 200.3655 | 200.6080 | 200.2390 | 200.0824 | 199.2450 |
| | <i>SDRL</i> | 198.3768 | 202.8921 | 203.3510 | 199.1435 | 202.0609 | 202.5535 |
| 0.1 | <i>ARL</i> | 193.0845 | 194.5760 | 196.0710 | 197.3380 | 197.9020 | 198.1715 |
| | <i>SDRL</i> | 193.3813 | 194.6717 | 197.0311 | 196.1353 | 196.4102 | 196.2692 |
| 0.2 | <i>ARL</i> | 190.5070 | 192.4800 | 192.6140 | 193.4525 | 194.0840 | 194.8685 |
| | <i>SDRL</i> | 190.1296 | 192.7278 | 192.8264 | 193.8498 | 194.8616 | 193.0579 |
| 0.3 | <i>ARL</i> | 172.3015 | 175.3870 | 176.4730 | 176.6070 | 177.6580 | 178.3040 |
| | <i>SDRL</i> | 172.2264 | 172.4015 | 177.3245 | 177.5226 | 177.9541 | 178.8112 |
| 0.50 | <i>ARL</i> | 131.0185 | 133.5100 | 135.3715 | 140.7375 | 141.9195 | 142.1545 |
| | <i>SDRL</i> | 128.4163 | 135.2401 | 135.4230 | 140.4510 | 141.8828 | 141.9179 |
| 0.75 | <i>ARL</i> | 75.2030 | 77.8200 | 80.5470 | 81.7215 | 85.1150 | 86.7445 |
| | <i>SDRL</i> | 74.9936 | 76.8780 | 80.6289 | 81.9079 | 86.6554 | 86.7219 |
| 1 | <i>ARL</i> | 33.0060 | 34.8290 | 37.5640 | 42.2255 | 43.5820 | 44.7785 |
| | <i>SDRL</i> | 32.8341 | 33.2356 | 37.4780 | 42.4154 | 42.5298 | 43.7556 |

Tab. 7. ARL and SDRL comparison under different error variance values in scenario 6

| δ | Criterion | UCL_{RPLRME} | | | | | |
|----------|-------------|-------------------------|----------------------------|---------------------------|----------------------------|---------------------------|----------------------------|
| | | 4.8104 | 5.1018 | 5.3913 | 5.6462 | 5.8613 | 6.0642 |
| | | $\sigma_\epsilon^2 = 0$ | $\sigma_\epsilon^2 = 0.05$ | $\sigma_\epsilon^2 = 0.1$ | $\sigma_\epsilon^2 = 0.15$ | $\sigma_\epsilon^2 = 0.2$ | $\sigma_\epsilon^2 = 0.25$ |
| 0 | <i>ARL</i> | 200.0270 | 200.3655 | 200.6080 | 200.2390 | 200.0824 | 199.2450 |
| | <i>SDRL</i> | 198.3768 | 202.8921 | 203.3510 | 199.1435 | 202.0609 | 202.5535 |
| 0.1 | <i>ARL</i> | 161.5690 | 163.1995 | 165.1805 | 167.5415 | 169.2515 | 173.2880 |
| | <i>SDRL</i> | 161.0361 | 161.1632 | 165.0655 | 165.9218 | 169.7752 | 170.2243 |
| 0.2 | <i>ARL</i> | 92.9490 | 97.9600 | 100.8430 | 108.2135 | 111.6610 | 116.5050 |
| | <i>SDRL</i> | 90.7152 | 94.7094 | 102.5694 | 110.6930 | 112.0497 | 119.9457 |
| 0.3 | <i>ARL</i> | 47.3150 | 51.8035 | 56.3675 | 63.0490 | 70.0625 | 70.6720 |
| | <i>SDRL</i> | 45.5090 | 51.2175 | 54.2517 | 60.3571 | 70.5067 | 71.1131 |
| 0.50 | <i>ARL</i> | 16.9195 | 18.9950 | 21.6200 | 23.5730 | 25.8125 | 29.3475 |
| | <i>SDRL</i> | 16.5987 | 17.9258 | 20.9726 | 21.9843 | 24.7490 | 28.3228 |
| 0.75 | <i>ARL</i> | 7.9120 | 8.7765 | 9.5920 | 10.8185 | 11.6465 | 12.9700 |
| | <i>SDRL</i> | 7.4869 | 8.5333 | 9.0608 | 10.2250 | 11.6724 | 12.5675 |
| 1 | <i>ARL</i> | 4.8110 | 5.3605 | 5.9730 | 6.3250 | 6.6520 | 7.4070 |
| | <i>SDRL</i> | 4.3165 | 4.8903 | 5.6324 | 5.7195 | 6.1936 | 6.7696 |

Tab. 8. ARL and SDRL comparison under different error variance values in scenario 7

| δ | Criterion | UCL_{RPLRME} | | | | | |
|----------|-------------|-------------------------|----------------------------|---------------------------|----------------------------|---------------------------|----------------------------|
| | | 4.8104 | 5.1018 | 5.3913 | 5.6462 | 5.8613 | 6.0642 |
| | | $\sigma_\epsilon^2 = 0$ | $\sigma_\epsilon^2 = 0.05$ | $\sigma_\epsilon^2 = 0.1$ | $\sigma_\epsilon^2 = 0.15$ | $\sigma_\epsilon^2 = 0.2$ | $\sigma_\epsilon^2 = 0.25$ |
| 0 | <i>ARL</i> | 200.0270 | 200.3655 | 200.6080 | 200.2390 | 200.0824 | 199.2450 |
| | <i>SDRL</i> | 198.3768 | 202.8921 | 203.3510 | 199.1435 | 202.0609 | 202.5535 |

| | | | | | | | |
|------|------|----------|----------|----------|----------|----------|----------|
| 0.1 | ARL | 194.6415 | 195.6575 | 196.3930 | 197.3485 | 198.6540 | 198.8185 |
| | SDRL | 194.8101 | 195.0791 | 196.1245 | 196.7619 | 197.5123 | 198.4807 |
| 0.2 | ARL | 186.2280 | 187.0325 | 187.6900 | 188.8865 | 190.4890 | 193.1945 |
| | SDRL | 187.8216 | 188.0193 | 188.0547 | 188.3663 | 188.1223 | 193.2670 |
| 0.3 | ARL | 175.7235 | 176.3475 | 177.5375 | 177.6245 | 178.0000 | 180.5335 |
| | SDRL | 172.5511 | 173.0896 | 176.6114 | 177.9696 | 180.3428 | 185.6862 |
| 0.5 | ARL | 127.3435 | 128.7440 | 138.7395 | 139.1250 | 139.5340 | 142.5995 |
| | SDRL | 124.6256 | 127.2070 | 135.4627 | 136.2119 | 137.9397 | 144.8344 |
| 0.75 | ARL | 80.9620 | 88.3155 | 93.7785 | 99.0500 | 106.7805 | 108.0015 |
| | SDRL | 75.2710 | 88.9093 | 89.6775 | 100.4935 | 104.9576 | 106.1982 |
| 1 | ARL | 55.9760 | 57.9725 | 64.5650 | 69.7905 | 70.2505 | 78.9680 |
| | SDRL | 56.2406 | 57.3907 | 60.9027 | 68.0019 | 68.1556 | 79.3262 |

In the rest of this section, according to section 3, we explore the performance of the RPLRMME chart in reducing the undesired impact of error contamination. We employ simulation experiments considering the same defined out-of-control scenarios when $\sigma_\varepsilon^2 = 0.25$. For this purpose, the performance of the RPLRME chart is compared to RPLRMME chart with $m = 2, 3, 5$ measurements per item in terms of *ARL* and *SDRL* and the results are summarized in Tables 9-15. The results reveal the superiority of the RPLRMME chart over the RPLRME one for both sparse or non-sparse shift patterns. That is to say, the delay in detection of sustained shifts caused by the error contamination can be adequately reduced when each item is measured several times. For more clarification, Figure 1 illustrates the percentage of *ARL* deterioration of the RPLRMME chart with $m = 1, 2, 3$ and 5 under the first out-of-control scenario for

$\delta \in \{0.1, 0.2, 0.3, 0.5, 0.75, 1\}$. For instance, in this scenario when $\delta = 0.5$, the *ARL* obtained by the RPLRMME chart with $m = 5$ is only 3.634663 percent larger than that of the no-error case. However, under single measurement condition, the mentioned difference increases to 42.62781 percent. This trend can be also observed for the other out-of-control scenarios. Besides, as indicated, the difference between with and without-error cases diminishes as the number of measurements per sampled item increases. In other words, for large values of m , the *ARL* values approach those obtained under no-error cases. The results of Tables 9-15 tell us that the run length properties of the RPLRMME chart with $m = 5$ inspections per sampled unit is approximately similar to those of no-error case. The same conclusions can be drawn when *SDRL* metric is taken into account.

Tab. 9. ARL and SDRL values when $\sigma_\varepsilon^2 = 0.25$ and $m \in \{1, 2, 3, 5\}$ in scenario 1

| δ | Criterion | $UCL_{RPLRMME}$ | | | | |
|----------|-----------|-----------------|----------|----------|----------|----------|
| | | 4.8104 | 6.0642 | 5.5185 | 5.2926 | 5.0970 |
| | | No error | $m = 1$ | $m = 2$ | $m = 3$ | $m = 5$ |
| 0 | ARL | 200.0270 | 199.2450 | 201.8091 | 199.0165 | 199.4916 |
| | SDRL | 198.3768 | 202.5535 | 199.1630 | 192.9853 | 197.2154 |
| 0.1 | ARL | 71.8085 | 96.1550 | 86.6425 | 81.5708 | 77.1850 |
| | SDRL | 69.2305 | 97.5912 | 87.4703 | 79.9065 | 76.7903 |
| 0.2 | ARL | 18.9235 | 30.4290 | 24.8424 | 22.1050 | 20.9198 |
| | SDRL | 18.5084 | 30.4888 | 24.2118 | 21.1159 | 20.5495 |
| 0.3 | ARL | 7.9315 | 13.4650 | 10.0922 | 9.3222 | 8.8524 |
| | SDRL | 7.5446 | 12.8001 | 9.5824 | 8.8027 | 8.3229 |
| 0.50 | ARL | 3.2080 | 4.5755 | 3.7839 | 3.5960 | 3.3246 |
| | SDRL | 2.6986 | 3.9587 | 3.2522 | 3.0572 | 2.7306 |
| 0.75 | ARL | 1.7765 | 2.2315 | 2.0240 | 1.9196 | 1.8548 |
| | SDRL | 1.2285 | 1.6713 | 1.4184 | 1.3039 | 1.2758 |
| 1 | ARL | 1.3030 | 1.5155 | 1.4167 | 1.4072 | 1.3562 |
| | SDRL | 0.6176 | 0.8923 | 0.7645 | 0.7402 | 0.6927 |

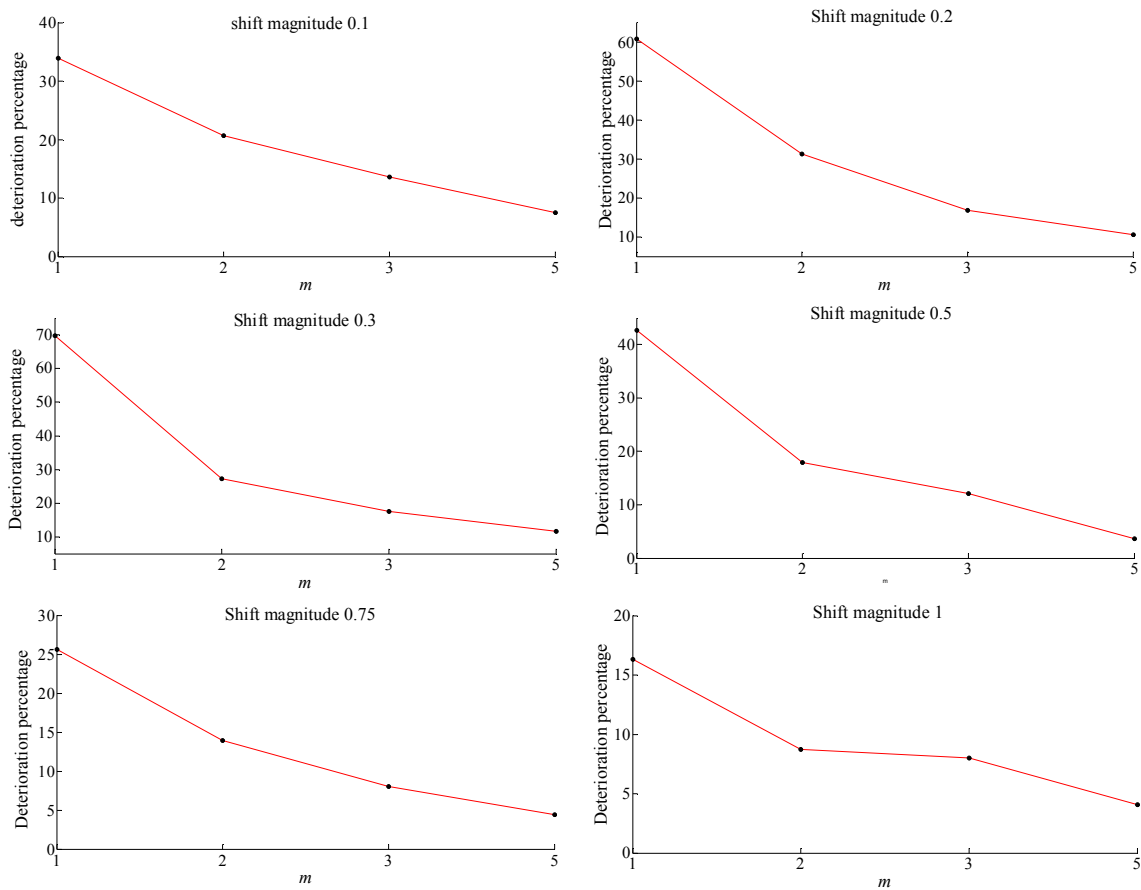


Fig. 1. Percentage of ARL deterioration in scenario 1

Tab. 10. ARL and SDRL values when $\sigma_e^2 = 0.25$ and $m \in \{1, 2, 3, 5\}$ in scenario 2

| δ | Criterion | UCI_{RPLRME} | | | | |
|----------|-----------|----------------|----------|----------|----------|----------|
| | | No error | $m = 1$ | $m = 2$ | $m = 3$ | $m = 5$ |
| 0 | ARL | 200.0270 | 199.2450 | 201.8091 | 199.0165 | 199.4916 |
| | SDRL | 198.3768 | 202.5535 | 199.1630 | 192.9853 | 197.2154 |
| 0.1 | ARL | 151.7150 | 165.6505 | 158.3782 | 153.7458 | 152.4110 |
| | SDRL | 156.9350 | 162.3510 | 157.8713 | 153.9333 | 151.4356 |
| 0.2 | ARL | 73.4590 | 97.8320 | 84.5340 | 79.8732 | 75.9162 |
| | SDRL | 75.5450 | 97.7902 | 83.4444 | 78.5593 | 74.7028 |
| 0.3 | ARL | 33.2720 | 49.7135 | 42.8334 | 39.3472 | 36.7922 |
| | SDRL | 33.1084 | 49.5135 | 42.6793 | 39.0212 | 36.3339 |
| 0.50 | ARL | 10.2085 | 15.7470 | 12.6740 | 11.8168 | 10.8622 |
| | SDRL | 9.6701 | 14.8825 | 12.2175 | 11.6006 | 10.2842 |
| 0.75 | ARL | 3.9700 | 5.7540 | 4.7766 | 4.4780 | 4.3406 |
| | SDRL | 3.3421 | 5.0501 | 4.2139 | 3.9376 | 3.8650 |
| 1 | ARL | 2.2880 | 3.0440 | 2.5774 | 2.4630 | 2.3534 |
| | SDRL | 1.7273 | 2.5104 | 1.9762 | 1.9489 | 1.7913 |

Tab. 11. ARL and SDRL values when $\sigma_\varepsilon^2 = 0.25$ and $m \in \{1, 2, 3, 5\}$ in scenario 3

| δ | Criterion | UCL_{RPLRME} | | | | |
|----------|-----------|----------------|----------|----------|----------|----------|
| | | 4.8104 | 6.0642 | 5.5185 | 5.2926 | 5.0970 |
| | | No error | $m = 1$ | $m = 2$ | $m = 3$ | $m = 5$ |
| 0 | ARL | 200.0270 | 199.2450 | 201.8091 | 199.0165 | 199.4916 |
| | SDRL | 198.3768 | 202.5535 | 199.1630 | 192.9853 | 197.2154 |
| 0.1 | ARL | 182.4620 | 194.8600 | 188.2894 | 193.7182 | 189.7958 |
| | SDRL | 177.0263 | 194.7752 | 186.8011 | 196.6489 | 189.5215 |
| 0.2 | ARL | 167.4450 | 175.1330 | 168.8866 | 167.0454 | 165.2840 |
| | SDRL | 167.1549 | 174.3643 | 172.8312 | 167.7489 | 168.3092 |
| 0.3 | ARL | 134.4550 | 143.0055 | 137.7388 | 131.2532 | 130.4826 |
| | SDRL | 131.0360 | 141.4138 | 138.1823 | 132.2029 | 131.7868 |
| 0.50 | ARL | 62.5985 | 78.3770 | 73.1550 | 67.8338 | 65.9210 |
| | SDRL | 64.5629 | 79.3273 | 71.1708 | 66.3890 | 65.5718 |
| 0.75 | ARL | 23.3575 | 32.3025 | 27.8096 | 25.3058 | 24.6116 |
| | SDRL | 22.7927 | 31.9370 | 27.5751 | 25.2759 | 24.2312 |
| 1 | ARL | 9.1005 | 13.9965 | 11.4574 | 10.5152 | 9.8968 |
| | SDRL | 8.6486 | 13.3382 | 10.6726 | 9.9103 | 9.5027 |

Tab. 12. ARL and SDRL values when $\sigma_\varepsilon^2 = 0.25$ and $m \in \{1, 2, 3, 5\}$ in scenario 4

| δ | Criterion | UCL_{RPLRME} | | | | |
|----------|-----------|----------------|----------|----------|----------|----------|
| | | 4.8104 | 6.0642 | 5.5185 | 5.2926 | 5.0970 |
| | | No error | $m = 1$ | $m = 2$ | $m = 3$ | $m = 5$ |
| 0 | ARL | 200.0270 | 199.2450 | 201.8091 | 199.0165 | 199.4916 |
| | SDRL | 198.3768 | 202.5535 | 199.1630 | 192.9853 | 197.2154 |
| 0.1 | ARL | 181.3370 | 187.4475 | 176.5550 | 176.4356 | 176.1178 |
| | SDRL | 184.0674 | 187.5506 | 176.9491 | 180.7028 | 179.2015 |
| 0.2 | ARL | 112.3760 | 123.8915 | 119.9202 | 115.9962 | 114.7818 |
| | SDRL | 111.1317 | 123.4841 | 119.8491 | 114.9623 | 116.0651 |
| 0.3 | ARL | 61.3020 | 70.8125 | 65.8958 | 65.6170 | 62.9370 |
| | SDRL | 61.0218 | 70.6627 | 65.1522 | 64.4477 | 60.6513 |
| 0.50 | ARL | 13.4815 | 18.7240 | 16.3666 | 14.6112 | 14.5450 |
| | SDRL | 12.8838 | 18.4422 | 15.8692 | 14.1536 | 14.1281 |
| 0.75 | ARL | 2.7455 | 3.8760 | 3.2512 | 3.1202 | 2.9294 |
| | SDRL | 2.1310 | 3.3017 | 2.6905 | 2.5754 | 2.3644 |
| 1 | ARL | 1.2635 | 1.5370 | 1.3878 | 1.3332 | 1.3272 |
| | SDRL | 0.5632 | 0.8860 | 0.7424 | 0.6520 | 0.6787 |

Tab. 13. ARL and SDRL values when $\sigma_\varepsilon^2 = 0.25$ and $m \in \{1, 2, 3, 5\}$ in scenario 5

| δ | Criterion | UCL_{RPLRME} | | | | |
|----------|-----------|----------------|----------|----------|----------|----------|
| | | 4.8104 | 6.0642 | 5.5185 | 5.2926 | 5.0970 |
| | | No error | $m = 1$ | $m = 2$ | $m = 3$ | $m = 5$ |
| 0 | ARL | 200.0270 | 199.2450 | 201.8091 | 199.0165 | 199.4916 |
| | SDRL | 198.3768 | 202.5535 | 199.1630 | 192.9853 | 197.2154 |
| 0.1 | ARL | 193.0845 | 198.1715 | 198.6568 | 196.0188 | 197.0706 |
| | SDRL | 193.3813 | 196.2692 | 206.0462 | 198.4430 | 197.4494 |
| 0.2 | ARL | 190.5070 | 194.8685 | 189.0488 | 191.8264 | 184.3404 |
| | SDRL | 190.1296 | 193.0579 | 182.9238 | 192.5177 | 180.7635 |
| 0.3 | ARL | 172.3015 | 178.3040 | 181.2012 | 176.5138 | 177.4280 |
| | SDRL | 172.2264 | 178.8112 | 182.3975 | 176.9453 | 181.9473 |
| 0.50 | ARL | 131.0185 | 142.1545 | 139.4750 | 135.4668 | 135.0024 |

| | | | | | | |
|------|-------------|----------|----------|----------|----------|----------|
| | <i>SDRL</i> | 128.4163 | 141.9179 | 140.3504 | 135.1690 | 134.2531 |
| 0.75 | <i>ARL</i> | 75.2030 | 86.7445 | 81.7062 | 80.5364 | 75.5910 |
| | <i>SDRL</i> | 74.9936 | 86.7219 | 82.5199 | 78.6665 | 74.3763 |
| 1 | <i>ARL</i> | 33.0060 | 44.7785 | 39.1652 | 36.2046 | 35.0308 |
| | <i>SDRL</i> | 32.8341 | 43.7556 | 39.1977 | 35.3549 | 33.8459 |

Tab. 14. ARL and SDRL values when $\sigma_\epsilon^2 = 0.25$ and $m \in \{1,2,3,5\}$ in scenario 6

| δ | Criterion | UCL_{RPLRME} | | | | |
|----------|-------------|----------------|----------|----------|----------|----------|
| | | 4.8104 | 6.0642 | 5.5185 | 5.2926 | 5.0970 |
| | | No error | $m = 1$ | $m = 2$ | $m = 3$ | $m = 5$ |
| 0 | <i>ARL</i> | 200.0270 | 199.2450 | 201.8091 | 199.0165 | 199.4916 |
| | <i>SDRL</i> | 198.3768 | 202.5535 | 199.1630 | 192.9853 | 197.2154 |
| 0.1 | <i>ARL</i> | 161.5690 | 173.2880 | 169.8004 | 166.4040 | 159.9754 |
| | <i>SDRL</i> | 161.0361 | 170.2243 | 170.2430 | 163.6367 | 160.6542 |
| 0.2 | <i>ARL</i> | 92.9490 | 116.5050 | 104.1308 | 97.7810 | 95.3758 |
| | <i>SDRL</i> | 90.7152 | 119.9457 | 103.0086 | 98.3814 | 95.3568 |
| 0.3 | <i>ARL</i> | 47.3150 | 70.6720 | 58.6210 | 55.0554 | 51.1696 |
| | <i>SDRL</i> | 45.5090 | 71.1131 | 58.9310 | 55.0585 | 49.8473 |
| 0.50 | <i>ARL</i> | 16.9195 | 29.3475 | 22.6900 | 20.7418 | 18.9808 |
| | <i>SDRL</i> | 16.5987 | 28.3228 | 22.1158 | 20.0225 | 18.2600 |
| 0.75 | <i>ARL</i> | 7.9120 | 12.9700 | 10.0642 | 9.4114 | 8.6334 |
| | <i>SDRL</i> | 7.4869 | 12.5675 | 9.4414 | 8.9387 | 8.1535 |
| 1 | <i>ARL</i> | 4.8110 | 7.4070 | 5.9632 | 5.4426 | 5.2198 |
| | <i>SDRL</i> | 4.3165 | 6.7696 | 5.4595 | 4.8168 | 4.6219 |

Tab. 15. ARL and SDRL values when $\sigma_\epsilon^2 = 0.25$ and $m \in \{1,2,3,5\}$ in scenario 7

| δ | Criterion | UCL_{RPLRME} | | | | |
|----------|-------------|----------------|----------|----------|----------|----------|
| | | 4.8104 | 6.0642 | 5.5185 | 5.2926 | 5.0970 |
| | | No error | $m = 1$ | $m = 2$ | $m = 3$ | $m = 5$ |
| 0 | <i>ARL</i> | 200.0270 | 199.2450 | 201.8091 | 199.0165 | 199.4916 |
| | <i>SDRL</i> | 198.3768 | 202.5535 | 199.1630 | 192.9853 | 197.2154 |
| 0.1 | <i>ARL</i> | 194.6415 | 198.8185 | 200.7230 | 189.8260 | 194.4568 |
| | <i>SDRL</i> | 194.8101 | 198.4807 | 197.2272 | 191.9087 | 194.7432 |
| 0.2 | <i>ARL</i> | 186.2280 | 193.1945 | 184.8002 | 182.3852 | 182.4656 |
| | <i>SDRL</i> | 187.8216 | 193.2670 | 184.1209 | 187.3233 | 181.2584 |
| 0.3 | <i>ARL</i> | 175.7235 | 180.5335 | 173.3552 | 169.0096 | 179.0492 |
| | <i>SDRL</i> | 172.5511 | 185.6862 | 172.8763 | 170.4638 | 180.5072 |
| 0.50 | <i>ARL</i> | 127.3435 | 142.5995 | 137.9468 | 137.6036 | 126.4556 |
| | <i>SDRL</i> | 124.6256 | 144.8344 | 137.6460 | 138.4305 | 126.1620 |
| 0.75 | <i>ARL</i> | 80.9620 | 108.0015 | 96.6572 | 92.2376 | 86.0044 |
| | <i>SDRL</i> | 75.2710 | 106.1982 | 95.6434 | 93.0626 | 86.9232 |
| 1 | <i>ARL</i> | 55.9760 | 78.9680 | 66.6894 | 63.7292 | 57.9780 |
| | <i>SDRL</i> | 56.2406 | 79.3262 | 64.8023 | 63.0132 | 58.2197 |

5. Conclusions and Future Directions

In this paper, we proposed a novel control chart based on the ridge penalized likelihood ratio statistic for Phase II monitoring of high-dimensional process variability taking the gauge impression into account. In contrast to the other control charts for covariance matrix monitoring under high-dimensionality, the proposed control chart relaxes the sparsity assumption of the covariance matrix. It means that on one hand, the developed chart can be used for monitoring both

sparse and non-sparse high-dimensional covariance matrix, on the other hand it can even detect sparse shifts in diagonal and/or off-diagonal covariance matrix elements. To compensate for the adverse effect of contamination due to the measurement errors, the RPLRME chart statistic was extended such that each item in a subgroup is inspected several times. To probe the efficiency of the proposed RPLRME chart, seven out-of-control scenarios including both sparse and non-sparse shifts in

high-dimensional covariance were defined. Then, extensive simulation studies in terms of the *ARL* and *SDRL* metrics were implemented to investigate how gauge inaccuracy deteriorates the sensitivity of the proposed chart in the detection of different anomalies in diagonal and/or off-diagonal elements. As expected, the results confirmed that the gauge's inability to accurately measure the process observations reduces the sensitivity of the developed control chart while employing multiple measurements approach can adequately compensate for the undesired impact of contaminated observations due to measurement errors. In other words, the detection capability of the developed RPLRMME chart approaches no-error case when the number of inspections per sampled item increases. The future studies can be extended in two directions: (1) developing control charts for monitoring the variability of the high-dimensional process with finite horizon productions, and (2) investigating the impact of estimation error on conditional *ARL* properties of the proposed RPLRME control chart.

References

- [1] Lim, J., & Lee, S. Phase II monitoring of changes in mean from high dimensional data. *Applied Stochastic Models in Business and Industry*, Vol. 33, No. 6, (2017), pp. 626-639.
- [2] Feng, L., Ren, H., & Zou, C. A setwise EWMA scheme for monitoring high-dimensional datastreams. *Random Matrices: Theory and Applications*, Vol. 9, No. 02, (2020), p. 2050004.
- [3] Ebrahimi, S., Ranjan, C., & Paynabar, K. Monitoring and root-cause diagnostics of high-dimensional data streams. *Journal of Quality Technology*, Vol. 54, No. 1, (2021), pp. 20-43.
- [4] Gunaratne, N. G. T., Abdollahian, M. A., Huda, S., & Yearwood, J. Exponentially weighted control charts to monitor multivariate process variability for high dimensions. *International Journal of Production Research*, Vol. 55, No. 17, (2017), pp. 4948-4962.
- [5] Abdella, G. M., Kim, J., Kim, S., Al-Khalifa, K. N., Jeong, M. K., Hamouda, A. M., & Elsayed, E. A. An adaptive thresholding-based process variability monitoring. *Journal of Quality Technology*, Vol. 51, No. 3, (2019), pp. 242-256.
- [6] Kim, J., Abdella, G. M., Kim, S., Al-Khalifa, K. N., & Hamouda, A. M. Control charts for variability monitoring in high-dimensional processes. *Computers & Industrial Engineering*, Vol. 130, (2019), pp. 309-316.
- [7] Abdella, G. M., Maleki, M. R., Kim, S., Al-Khalifa, K. N., & Hamouda, A. M. S. Phase-I monitoring of high-dimensional covariance matrix using an adaptive thresholding LASSO rule. *Computers & Industrial Engineering*, Vol. 144, (2020), pp. 106465.
- [8] Fan, J., Shu, L., Yang, A., & Li, Y. Phase I analysis of high-dimensional covariance matrices based on sparse leading eigenvalues. *Journal of Quality Technology*, Vol. 53, No. 4, (2021), pp. 333-346.
- [9] Saemian, M., Salmasnia, A., & Maleki, M. R. A generalized multiple dependent state sampling chart based on ridge penalized likelihood ratio for high-dimensional covariance matrix monitoring. *Scientia Iranica*, In Press, (2023).
- [10] Jafari, M., Maleki, M. R., & Salmasnia, A. A high-dimensional control chart for monitoring process variability under gauge imprecision effect. *Production Engineering*, Vol. 17, (2023), pp. 547-564.
- [11] Salmasnia, A., Maleki, M. R., & Mirzaei, M. Double Sampling Adaptive Thresholding LASSO Variability Chart for Phase II Monitoring of High-Dimensional Data Streams. *Journal of Industrial Integration and Management*, In Press, (2023).
- [12] Maleki, M. R., & Salmasnia, A. Joint Monitoring of Process Location and Dispersion Based on CUSUM Procedure and Generalized Likelihood Ratio in the Presence of Measurement Errors. *Quality*

- and Reliability Engineering International*, Vol. 33, No. 7, (2017), pp. 1485-1498.
- [13] Salmasnia, A., Maleki, M. R., & Niaki, S. T. A. Remedial measures to lessen the effect of imprecise measurement with linearly increasing variance on the performance of the MAX-EWMAMS scheme. *Arabian Journal for Science and Engineering*, Vol. 43, No. 6, (2018), pp. 3151-3162.
- [14] Khalafi, S., Salmasnia, A., & Maleki, M. R. Remedial approaches to decrease the effect of measurement errors on simple linear profile monitoring. *International Journal for Quality Research*, Vol. 14, No. 4, (2020).
- [15] Nguyen, H. D., Tran, K. P., & Tran, K. D. The effect of measurement errors on the performance of the Exponentially Weighted Moving Average control charts for the Ratio of Two Normally Distributed Variables. *European Journal of Operational Research*, Vol. 293, No. 1, (2021), pp. 203-218.
- [16] Saha, S., Khoo, M. B., Castagliola, P., & Haq, A. Side sensitive modified group runs charts with and without measurement errors for monitoring the coefficient of variation. *Quality and Reliability Engineering International*, Vol. 37, No. 2, (2021), pp. 598-617.
- [17] Saemian, M., Maleki, M. R. Salmasnia, A. Performance of Max-HEWMAMS control chart for simultaneous monitoring of process mean and variability in the presence of measurement errors, *International Journal of Applied Decision Sciences*, In Press, (2022).
- [18] Sabahno, H., Amiri, A., & Castagliola, P. Evaluating the effect of measurement errors on the performance of the variable sampling intervals Hotelling's T^2 control charts. *Quality and Reliability Engineering International*, Vol. 34, No. 8, (2018), pp. 1785-1799.
- [19] Zaidi, F. S., Castagliola, P., Tran, K. P., & Khoo, M. B. C. Performance of the hotelling T^2 control chart for compositional data in the presence of measurement errors. *Journal of Applied Statistics*, Vol. 46, No. 14, (2019), pp. 2583-2602.
- [20] Nguyen, Q. T., Giner-Bosch, V., Tran, K. D., Heuchenne, C., & Tran, K. P. One-sided variable sampling interval EWMA control charts for monitoring the multivariate coefficient of variation in the presence of measurement errors. *The International Journal of Advanced Manufacturing Technology*, Vol. 115, (2021), pp. 1821-1851.
- [21] Maleki, M. R., Ghashghaei, R., & Amiri, A. Simultaneous monitoring of multivariate process mean and variability in the presence of measurement error with linearly increasing variance under additive covariate model (research note). *International Journal of Engineering*, Vol. 29, No. 4, (2016), pp. 514-523.
- [22] Amiri, A., Ghashghaei, R., & Maleki, M. R. On the effect of measurement errors in simultaneous monitoring of mean vector and covariance matrix of multivariate processes. *Transactions of the Institute of Measurement and Control*, Vol. 40, No. 1, (2018), pp. 318-330.
- [23] Zaidi, F. S., Castagliola, P., Tran, K. P., & Khoo, M. B. C. Performance of the MEWMA CoDa control chart in the presence of measurement errors. *Quality and Reliability Engineering International*, Vol. 36, No. 7, (2020), pp. 2411-2440.
- [24] Ayyoub, H. N., Khoo, M. B., Lee, M. H., & Haq, A. Monitoring multivariate coefficient of variation with upward Shewhart and EWMA charts in the presence of measurement errors using the linear covariate error model. *Quality and Reliability Engineering International*, Vol. 37, No. 2, (2021), pp. 694-716.
- [25] Yousefi, S., Maleki, M. R. Salmasnia, A. Kiani Anbohi, M. On the performance of multivariate homogeneously weighted moving average chart for monitoring the process mean in the presence of

- measurement errors. *Journal of Advanced Manufacturing Systems*, Vol. 22, No. 01, (2023), pp. 27-40.
- [26] Maleki, M. R., Amiri, A., & Castagliola, P. Measurement errors in statistical process monitoring: A literature review. *Computers & Industrial Engineering*, Vol. 103, (2017), pp. 316-329.
- [27] Linna, K. W., & Woodall, W. H. Effect of measurement error on Shewhart control charts. *Journal of Quality Technology*, Vol. 33, No. 2, (2001), pp. 213-222.
- [28] Ghashghaei, R., Bashiri, M., Amiri, A., & Maleki, M. R. Effect of measurement error on joint monitoring of process mean and variability under ranked set sampling. *Quality and Reliability Engineering International*, Vol. 32, No. 8, (2016), pp. 3035-3050.
- [29] Noor-ul-Amin, M., Javaid, A., Hanif, M., & Dogu, E. Performance of maximum EWMA control chart in the presence of measurement error using auxiliary information. *Communications in Statistics-Simulation and Computation*, Vol. 51, No. 9, (2022), pp. 5482-5506.
- [30] Maleki, M. R. Salmasnia, A., Yarmohammadi, S. The Performance of Triple Sampling \bar{X} Control Chart with Measurement Errors, *Quality Technology & Quantitative Management*, Vol. 19, No. 5, (2022), pp. 587-604.

Follow this article at the following site:

Esmail Safikhani, Ali Salmasnia & Mohammad Reza Maleki: A ridge penalized likelihood ratio chart for phase II monitoring of high-dimensional process dispersion under measurement system inaccuracy. *IJIEPR* 2023; 34 (2) :1-17
URL: <http://ijiepr.iust.ac.ir/article-1-1501-en.html>

